Apoptosis (2008) 13:295–304
DOI 10.1007/s10495-007-0160-y

ORIGINAL PAPER

Acetylcholine inhibits long-term hypoxia-induced apoptosis by suppressing the oxidative stress-mediated MAPKs activation as well as regulation of Bcl-2, c-IAPs, and caspase-3 in mouse embryonic stem cells

Min Hee Kim · Mi Ok Kim · Jung Sun Heo · Jin Sang Kim · Ho Jae Han

Published online: 30 November 2007

Abstract This study examined the effect of acetylcholine (ACh) on the hypoxia-induced apoptosis of mouse embryonic stem (ES) cells. Hypoxia (60 h) decreased both the cell viability and level of [^{3}H] thymidine incorporation, which were prevented by a pretreatment with ACh. However, the atropine (ACh receptor [AChR] inhibitor) treatment blocked the protective effect of ACh. Hypoxia (90 min) increased the intracellular level of reactive oxygen species (ROS). On the other hand, ACh inhibited the hypoxia-induced increase in ROS, which was blocked by an atropine treatment. Subsequently, the hypoxia-induced ROS increased the level of p38 mitogen activated protein kinase (MAPK) and Jun-N-terminal kinase (JNK) phosphorylation, which were inhibited by the ACh pretreatment. Moreover, hypoxic exposure (90 min) increased the level of nuclear factor-κB (NF-κB) phosphorylation, which was blocked by a pretreatment with SB 203580 (p38 MAPK inhibitor) or SP 600125 (JNK inhibitor). However, hypoxia (60 h) decreased the protein levels of Bcl-2 and c-IAPs (cellular inhibitor of apoptosis proteins) but increased the level of caspase-3 activation. All these effects were inhibited by a pretreatment with ACh. In conclusion, ACh prevented the hypoxia-induced apoptosis of mouse ES cells by inhibiting the ROS-mediated p38 MAPK and JNK activation as well as the regulation of Bcl-2, c-IAPs, and caspase-3.

Keywords Acetylcholine · Apoptosis · Embryonic stem cell · Hypoxia

Introduction

Oxygen is the most important factor in all forms of life [1]. Therefore, a change in the oxygen concentration induces a variety of cellular responses including changes in gene expression, metabolic function, ion channel activation, and the release of neurotransmitters [2, 3]. In particular, hypoxia elicits energy depletion, the release of excitatory amino acids, the accumulation of ROS, and initiation of apoptosis [4]. The generation of ROS by hypoxia provokes a variety of signal molecules such as MAPKs, which induce cell apoptosis [5]. Traditionally, the embryotoxicity induced by hypoxia was assumed to be necrotic because of the correlation between the energy failure and necrotic cell death [6]. The survival of ES cells is not only important for normal development that apoptosis in embryos is triggered by oxygen deprivation through the activation of effecter caspases [7].

ACh is widely distributed in pro- and eukaryotic organisms as well as in various non-nervous tissues of animals [8]. Cholinergic mechanisms have been implicated in the growth and maturation of oocytes in various species

Electronic supplementary material The online version of this article (doi:10.1007/s10495-007-0160-y) contains supplementary material, which is available to authorized users.

M. H. Kim
Department of Rehabilitation Science, Graduate school of Daegu University, Daegu 705-714, Korea

M. O. Kim · J. S. Heo · H. J. Han (✉)
Department of Veterinary Physiology, Biotherapy Human Resources Center (BK 21), College of Veterinary Medicine, Chonnam National University, Gwangju 500-757, Korea
e-mail: hjhan@chonnam.ac.kr

J. S. Kim
Department of Physical Therapy, College of Rehabilitation Science, Daegu University, Daegu 705-714, Korea

[9]. In addition, the expression of the cholinergic system during embryonic development is a widespread phenomenon [10]. However, it is unclear how the cholinergic system influences ES cells and its specific functions are not completely understood. ACh might function in the context of a classical neurotransmitter triad, which are ACh, AChR, and ACh esterase, and employ this triad to regulate the cell functions such as proliferation, differentiation, and the establishment of the cell–cell contacts [11, 12]. Among these functions, the proliferative effects of ACh have been demonstrated in various cell types, e.g., epithelial cells, thymocytes, or glial cells [13], and this process can be mediated by the AChR, which is coupled to the second messenger pathways. In addition, AChR exerts a modulatory role mainly in embryos and their cellular effects [12, 14]. ACh also protects neurons from a variety of insults both in vitro [15] and in vivo [16]. Although there are a few reports documenting ACh is involved in embryonic development [12, 17], a precise function has not been elucidated.

ES cells have the ability to differentiate into all three germ layers and have unlimited growth potential under certain conditions [18]. In vitro studies using a stem cell population with mammalian blastocysts have provided a powerful tool for analyzing the hypoxic effects on the cellular function [19]. The survival of ES cells is not only important for normal development in vivo but is also essential for the safe manipulation of cells under stressful conditions. This model will be helpful for understanding the effect of a low-oxygen environment in mouse ES cells [20]. Although few preliminary studies have implicated the neuroprotective potential of ACh against transient hypoxia [21, 22], the precise mechanisms of cell death and embryonic protection in ES cells are not completely understood. Therefore, this study examined the nature of cell apoptosis induced by long-term hypoxic exposure in mouse ES cells and assessed the ES cell protective potential of ACh.

Materials and methods

Materials

Mouse ES cells (ES-E14TG2a) were obtained from the American Type Culture Collection (Manassas, VA, USA). The experiments were carried out using ES-E14TG2a, except where indicated. Fetal bovine serum was purchased from Biowhittaker (Walkersville, MD, USA). Acetylcholine chloride was supplied by Sigma Chemical Company (St. Louis, MO, USA). SB 203580 and SP 600125 were obtained from the Sigma Chemical Company (St. Louis, MO, USA). Phospho-p38 MAPK, p38 MAPK, phospho-JNK, JNK, phospho-NF-κB, and NF-κB antibodies were purchased from New England Biolabs (Herts, UK). Bcl-2, c-IAP1, c-IAP2, and caspase-3 were purchased from Santa Cruz Biotechnology (Delaware, CA, USA). Goat anti-rabbit IgG and goat-anti mouse IgG were obtained from Jackson Immunoresearch (West Grove, PA, USA). All other reagents were purchased commercially and were of the highest purity available.

ES cell culture

The mouse ES cells were incubated in DMEM (Gibco-BRL, Gaithersburg, MD) supplemented with 3.7 g/l sodium bicarbonate, 1% penicillin and streptomycin, 1.7 mM L-glutamine, 0.1 mM β-mercaptoethanol, 5 ng/ml mouse leukemia inhibitory factor, and 15% fetal bovine serum (FBS) without a feeder layer for 5 days. The cells were grown on a gelatinized 35 or 60 mm culture dish in an incubator maintained at 37°C in an atmosphere containing 5% CO_2 in air. After 1–3 days, the cells were washed twice with phosphate-buffered saline (PBS) and maintained in serum-free DMEM including all the supplements. The resulting cells were used for the experiments after a 24 h incubation period.

Hypoxic treatment of ES cells

The ES cells were cultured in 35 or 60 mm culture dishes and washed twice with PBS. Subsequently, the media was changed to fresh serum-free DMEM supplemented with LIF. The experiments were carried our in an incubator at 37°C under normoxic conditions by maintaining the cells in an atmosphere containing 5% CO_2 in air or under hypoxic conditions by incubating cells in a modular incubator chamber gassed with 2.2% O_2, 5.5% CO_2, and 92.3% N_2 (Billups-Rptheberg Inc, CA, USA) at a flow rate of 20 l/min for 30 min. After the chamber was purged with gas, it was sealed and placed in a conventional incubator at 37°C during 60 h or 90 min.

Alkaline phosphatase (AP) staining

The mouse ES cells were washed twice with PBS and fixed with 4% formaldehyde (in PBS) for 15 min at room temperature. The cells were washed with PBS and incubated with an alkaline phosphatase substrate solution (200 μg/ml naphthol AS-MX phosphate, 2% *N*,*N*-dimethylformamide 0.1 M Tris [pH 8.2], and 1 mg/ml Fast Red TR salt [4-chloro-2-methylbenzenediazonium salt; zinc chloride]) for 10 min at room temperature. The cells were washed with PBS and photographed.

RNA isolation and RT-PCR

The total RNA was obtained from the mouse ES cells using STAT-60, monophasic solution of phenol and guanidine isothiocyanate from Tel-test, Inc (Firendwood, Tex., USA). Reverse transcription (RT) was carried out with 3 μg RNA using a reverse transcription system kit (AccuPower RT PreMix, Bioneer, Daejeon, Korea) with the oligo$(dT)_{18}$ primers. About 5 μl of the RT products was then amplified using a polymerase chain reaction (PCR) kit (AccuPower PCR Premix) under the following conditions: denaturation at 94°C for 5 min and 30 cycles at 94°C for 45 s, 55°C for 30 s, and 72°C for 30 s, followed by 5 min of extension at 72°C. The primers used were 5′-CGTGAGACTTTGCAG CCTGA-3′ (sense), 5′-GGCGATGTAAGTGATCTGCTG-3′ (antisense) for Oct4 (519 base pair [bp]); 5′-TCTTAC-ATCGCGCTCATCAC-3′ (sense), 5′-TCTTGACGAAGC AGTCGTTG-3′ (antisense) for FOXD3 (171 bp); 5′-GTGG AAACTTTTGTCCGAGAC-3′ (sense), 5′-TGGAGTGG-GAGGAAGAGGTAAC-3′ (antisense) for SOX2 (550 bp). PCR for β-actin was also carried out as a control for the RNA quantity.

Trypan blue exclusion test and lactate dehydronase (LDH) assay

In order to determine the number of cells, the cells were washed twice with PBS and trypsinized from the culture dishes. The cell suspension was mixed with a 0.4% (wt/vol) trypan blue solution (500 μl), and the number of live cells was determined using a hemocytometer. The cells failing to exclude the dye were considered nonviable. The level of cell injury was assessed using the LDH activity. The level of LDH activity in the medium was measured using a LDH assay kit (Iatron Lab, Tokyo, Japan). The level of LDH released is expressed as a percentage of the control (normoxia).

[^{3}H] thymidine incorporation

The [^{3}H] thymidine incorporation experiments were carried out using the methodology reported by Chen et al. [23] and Zhang et al. [24] that most ES cells could be arrested in the G0/G1 phase through serum deprivation. Furthermore, the synchronized ES cells could successfully reenter a normal cell cycle after being resupplied with serum. In this study, the cells were cultured in one well until they reached 50% confluence. The cells were then washed twice with PBS and maintained in serum free DMEM including all the supplements. After 24 h incubation, the cells were washed twice with PBS, and incubated with fresh serum free DMEM including all the supplements and the indicated agents. After the indicated incubation period, 1 μCi of [methyl-^{3}H] thymidine (specific activity: 74 GBq/mmol, 2.0 Ci/mmol; Amersham Biosciences, Buckinghamshire, UK) was added to the cultures and incubated for 1 h at 37°C. The cells were then washed twice with PBS, fixed in 10% trichloroacetic acid (TCA) at 23°C for 15 min, and washed twice with 5% TCA. The acid-insoluble material was dissolved in 0.2 N NaOH over a 12 h period at 23°C. Aliquots were removed, and the level of radioactivity was determined using a liquid scintillation counter (LS 6500, Beckman Instruments, Fullerton, CA). The control levels of [^{3}H] thymidine incorporation were determined under the conditions where the cells were cultured in serum free DMEM under normoxic conditions. The values were converted from the absolute counts to a percentage of the control in order to allow a comparison between the experimental groups.

DNA fragmentation assay

The semi-confluent mouse ES cells in a 60 mm dish were harvested after treating cells with the indicated conditions, then suspended in a lysis buffer (10 mM/l Tris–HCl [pH 7.5], 10 mM/l EDTA [pH 8.0], 0.5% Triton-X). The cell lysates were treated with 200 μg/ml proteinase K at 60°C for 6 h followed by DNA extraction using phenol-chloroform. The DNA extracted was precipitated using isopropyl alcohol, and then digested with 10 μg/ml TE-RNase at 37°C for 1 h. After digestion, the product was electrophoresed on 1% agarose gel stained with ethidium bromide and photographed under ultraviolet (UV) light.

Flow cytometry analysis

The cells were incubated with or without ACh under hypoxic conditions for 60 h, and the cells were then dissociated in trypsin/EDTA, pelleted by centrifugation, washed in PBS and fixed at 4°C in 70% ethanol for 12 h. The cells were then resuspended in PBS containing 0.1% BSA. When required, a PI solution (500 μg/ml PI in 3.8×10^{-2} M sodium citrate, [pH 7.0]) and boiled RNase (10 mg/ml prepared in 10 mM Tris–HCl, [pH 7.5]) were added to the cells in the dark at room temperature, and the cells were incubated 37°C for 30 min. The sample was read by flow cytometry and analyzed using CXP software (Beckman Coulter).

Assay of intracellular ROS

CM-H_2DCFDA (DCF-DA), which acts as a H_2O_2-sensitive fluorophore, was used to detect the ROS. About 10 μM

DCF-DA was added to cells, which were then incubated in the dark for 30 min at room temperature. The cells were then viewed using laser confocal microscopy (400×, fluoview 300, Olympus, Japan), the fluorescence was excited at 488 nm, and the light emitted was observed at 515–540 nm. In order to quantify the intracellular H_2O_2 levels, the cells treated with DCF-DA were rinsed twice with ice-cold PBS and then scraped. A 100 μl cell suspension was loaded into a 96-well plate and examined using a luminometer (Victor3, Perkinelmer, USA) and a fluorescent plate reader at excitation and emission wavelengths of 485 and 535 nm, respectively.

Western blot analysis

The cells were harvested, washed twice with PBS, and lysed with a buffer (137 mM NaCl, 8.1 mM Na_2HPO_4, 2.7 mM KCl, 1.5 mM KH_2PO_4, 2.5 mM EDTA, 1 mM dithiothreitol, 0.1 mM PMSF, 10 μg/ml leupeptin [pH 7.5]) for 30 min on ice. The lysates were centrifuged at 15,000 rpm for 10 min at 4°C, and the protein concentration was determined using the Bradford method [25]. Equal amounts of the protein (40 μg) were resolved by 10% SDS-polyacrylamide gel electrophoresis and transferred to nitrocellulose membranes. The blots on the membrane were washed with TBST (10 mM Tris–HCl [pH 7.6], 150 mM NaCl, 0.05% Tween 20), blocked with 5% skim milk for 1 h, and incubated with the appropriate primary antibody at the dilutions recommended by the supplier. The membrane was washed, and the primary antibodies were detected using goat anti-rabbit IgG or goat-anti mouse IgG conjugated to horseradish peroxidase. The bands were then visualized by enhanced chemiluminescence (Amersharm Pharmacia Biotech).

Statistical analysis

The results are expressed as a mean ± standard errors (SE). All the experiments were analyzed by analysis of variance, and some experiments were examined by a comparison of the treatment means with the control using the Bonferroni–Dunn test. The difference was considered statistically significant when $p < 0.05$.

Results

The protective effect of ACh on hypoxia-induced cell apoptosis

The undifferentiated state of the mouse ES cells used in this experiment was confirmed by examining the undifferentiated stem cells markers, which included the Oct-4, SOX-2 and FOXD3 gene expression levels as well as the alkaline phosphatase activity. As shown in Fig. 1A and B, the mouse ES cells maintained an undifferentiated state under the following conditions: normoxia, hypoxia, and ACh with hypoxia.

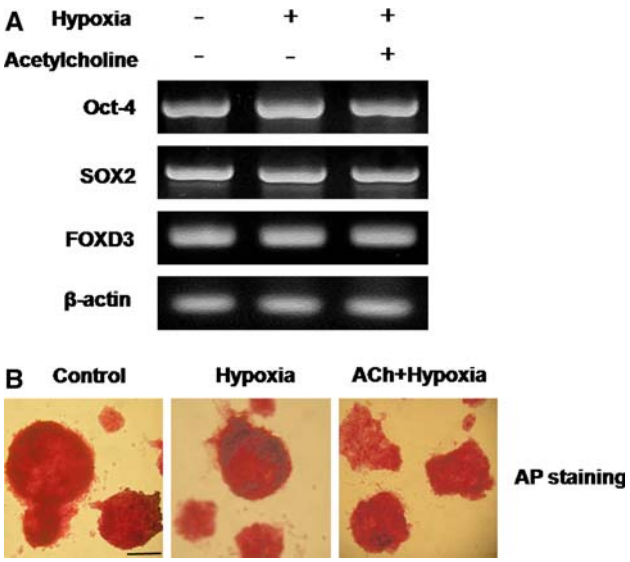

Fig. 1 Effect of hypoxia with or without ACh on the characterization of mouse ES cells. (**A**) Oct4 (519 bp), SOX 2 (550 bp), FOXD 3 (171 bp), and β-actin (350 bp) mRNA expression levels was examined in hypoxia with or without ACh (10^{-3} M) using RT-PCR. (**B**) The alkaline phosphatase enzyme activity was measured in the cells after 60 h of hypoxia, as described in Materials and Methods. The examples are representative of 3 independent experiments

In order to examine the effect of ACh and AChR on hypoxia-induced cell apoptosis, the cells were pretreated with ACh and atropine before being exposed to hypoxia for 60 h. As shown in Fig. 2A and B, the pretreatment with ACh (10^{-3} M) inhibited the hypoxia-induced decrease in the cell viability and the increase in the level of LDH released, which is a marker of structural damage. A pretreatment with atropine (AChR inhibitor, 10^{-3} M) inhibited the ACh-induced prevention of the hypoxic effect. Moreover, the hypoxia-induced decrease in the level of [^{3}H] thymidine incorporation was recovered by a pretreatment with ACh (Fig. 2C). Hypoxic exposure increased the level of fragmented DNA, which was protected by a pretreatment with ACh. However, atropine inhibited the protective effect of ACh (Fig. 2D). Flow cytometry analysis also showed that hypoxia increased the level of apoptotic cell death (Hypoxia: 37.5% vs. control: 8.06%). However, a pretreatment with ACh inhibited the hypoxic effect (23.7%) (Fig. 2E).

Effect of ACh on hypoxia-induced ROS generation

In order to examine the effect of ACh on the hypoxia-induced generation of ROS, the cells were pretreated with

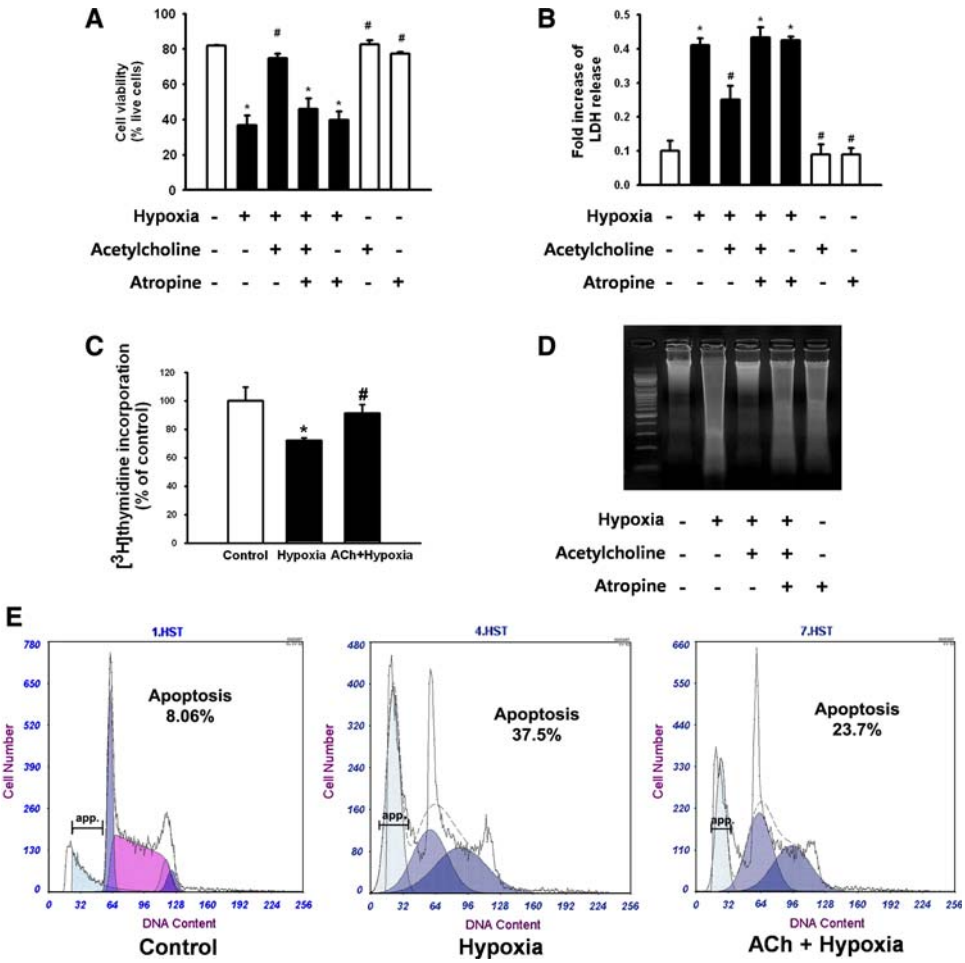

Fig. 2 Effect of ACh on the hypoxia-induced apoptotic cell death. The mouse ES cells with ACh or atropine were exposed to hypoxia for 60 h and (**A**) the cell viability and (**B**) LDH release was measured as described in Materials and methods. (**C**) Mouse ES cells with or without ACh were exposed to hypoxia for 60 h and pulsed with 1 μCi of [^{3}H] thymidine for 1 h before counting. (**D**) DNA fragmentation was assessed after 60 h hypoxia with ACh or the atropine pretreatment. (**E**) Flow cytometry analysis was assessed to confirm the hypoxia-induced apoptosis under hypoxia with or without ACh, as described Materials and methods. The values are reported as the mean ± SE of 3 independent experiments with triplicate dishes. Open bar, control; filled bars, hypoxia. * $P < 0.05$ versus control (normoxia), # $P < 0.05$ versus hypoxia alone

ACh before being exposed to 60 h of hypoxia. As shown in Fig. 3A, hypoxia increased the intracellular ROS levels but ACh inhibited this effect. Moreover, the cells were pre-treated with atropine (10^{-3} M) before hypoxic exposure in order to determine the effect of ACh via AChR on the hypoxia-induced generation of ROS. As shown in Fig. 3B, atropine abolished the inhibitory effect of ACh on the hypoxia-induced generation of ROS.

Effect of ACh on hypoxia-induced phosphorylation of MAPKs and NF-κB

In the experiment to examine the involvement of MAPKs in hypoxia-induced apoptotic cell death, hypoxia increased the level of p38 MAPK and JNK phosphorylation in a time-dependent manner (Fig. 4A). On the other hand, the hypoxia-induced phosphorylation of MAPKs was inhibited by a pretreatment with ACh. Moreover, the hypoxia-induced phosphorylation of p38 MAPK and JNK was inhibited by a pretreatment with antioxidants, vitamin C (10^{-3} M) and vitamin E (10^{-5} M) (Fig. 4B, C). In the next experiment, the level of NF-κB phosphorylation was increased from 30 min of hypoxic exposure in a time-dependent manner, and reached a maximum after 90 min of hypoxia (Fig. 5A). However, a pretreatment with ACh decreased the hypoxia-induced phosphorylation of NF-κB. The hypoxia-induced phosphorylation of NF-κB was also attenuated by a pretreatment with SB 203580 (10^{-6} M) and SP 600125 (10^{-6} M) (Fig. 5B).

Effect of hypoxia on Bcl-2, c-IAPs, and caspase-3 expressions

In experiments to examine the effect of hypoxia on the expression of Bcl-2 and c-IAPs, the levels of the Bcl-2, c-IAP1, and c-IAP2 proteins were increased up to 48 h, but

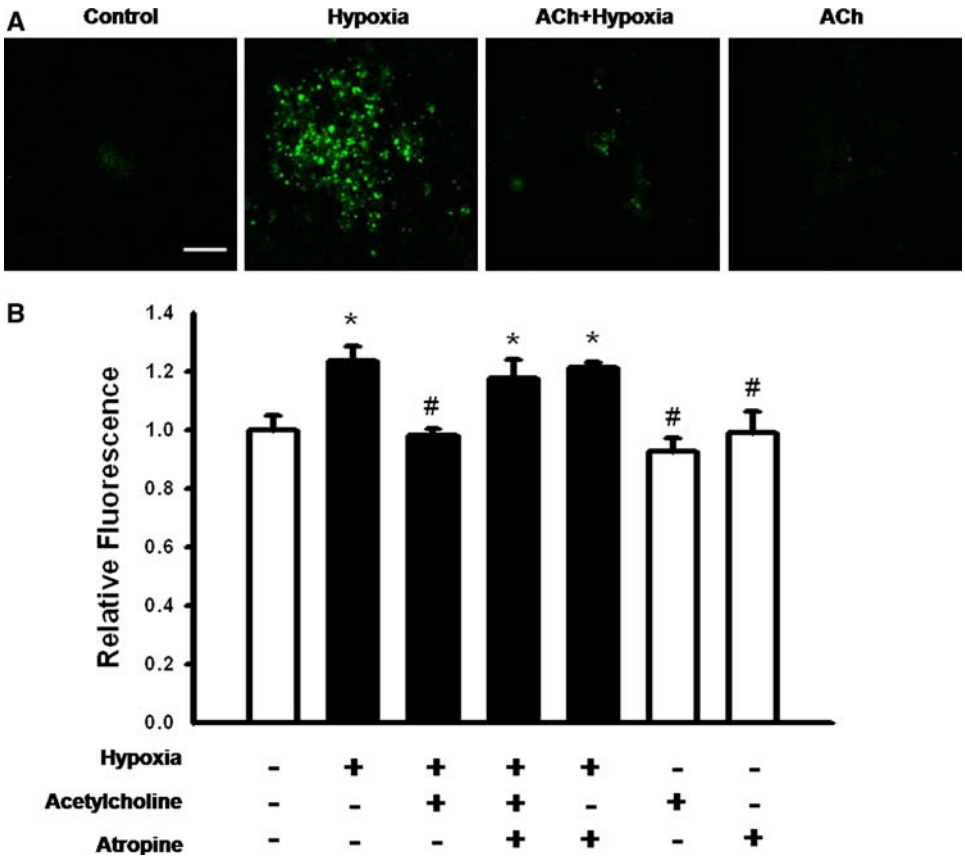

Fig. 3 Effect of ACh on the hypoxia-induced increase in ROS. (**A**) Mouse ES cells with or without ACh were exposed to hypoxia and the DCF fluorescence was measured. (**B**) The cells were pretreated with atropine (10^{-3} M) for 30 min before the ACh treatment, and exposed to hypoxia for 90 min. The values are reported as the mean ± SE of 3 independent experiments with triplicate dishes. Open bar, control; filled bars, hypoxia. * $P < 0.05$ versus control (normoxia), # $P < 0.05$ versus hypoxia alone

they had decreased after 60 h of hypoxia (Fig. 6A). However, a pretreatment with ACh prevented the decrease in the Bcl-2 and c-IAPs levels after 60 h of hypoxic exposure. Moreover, a pretreatment with BAY11-7082 (IκB phosphorylation inhibitor, 2×10^{-5} M) or SN 50 (NF-κB nucleus translocation inhibitor, 500 ng/ml) also inhibited the effect of hypoxia on these proteins (Fig. 6B, C, D). The level of caspase-3 activation was determined by monitoring the decrease in the level of the p32 precursor and the increase in the cleaved fragment p20 and p17 subunits. As shown in Fig. 7, the cleaved fragments, p20 and p17 subunits, were increased by hypoxia, but a pretreatment with ACh inhibited the activation of caspase-3.

Discussion

In this study, ACh inhibited the hypoxia-induced apoptosis by inhibiting the ROS-mediated p38 MAPK, JNK, and NF-κB pathways and regulating Bcl-2, c-IAPs, and caspase-3. The mechanism for this process must have a rapid onset and initiate a process that is maintained even after ACh has been withdrawn. Generally, the ACh concentration of whole blood is approximately 8.65 nM (1264 ± 149 pg/ml) in humans and 1.43 nM (209 ± 29 pg/ml) in rats [26]. However, ACh maintains high concentration during maturation and development of the placenta and the fetus, and is decreased by aging [27]. Moreover, a high ACh concentration is more effective to protect against the oxidative stress and the apoptotic process [28]. Therefore, in present study, we used higher concentration of ACh (1 mM) than the physiological level, which is consistent with previous studies [29, 30]. When considering the possible mechanisms for cell survival mediated by ACh, it is important to note that ACh is essential for protecting mouse ES cells from oxidative stress. ACh is also well known to have an anti-apoptotic effect via the increase of antioxidant action and the activation of survival signaling molecules, which are induced by AChR activation in various cell types [31–33]. Moreover, previous study showed that cholinergic system including muscarinic AChR (mAChR) expressed in mouse ES cells [12]. Therefore, it can be suggested that ACh/AChR is implicated to play an important role in ES cell expansion. However, the signal transduction pathways modulated by ACh to suppress the hypoxia-induced ES cell injury, or more specifically apoptosis, are largely unknown.

Under physiological conditions, the mitochondrial membrane is polarized and has a membrane potential, which is maintained by ATP and proton gradients across the membrane. These in turn are dependent on oxygen availability. Maintenance of membrane potential keeps

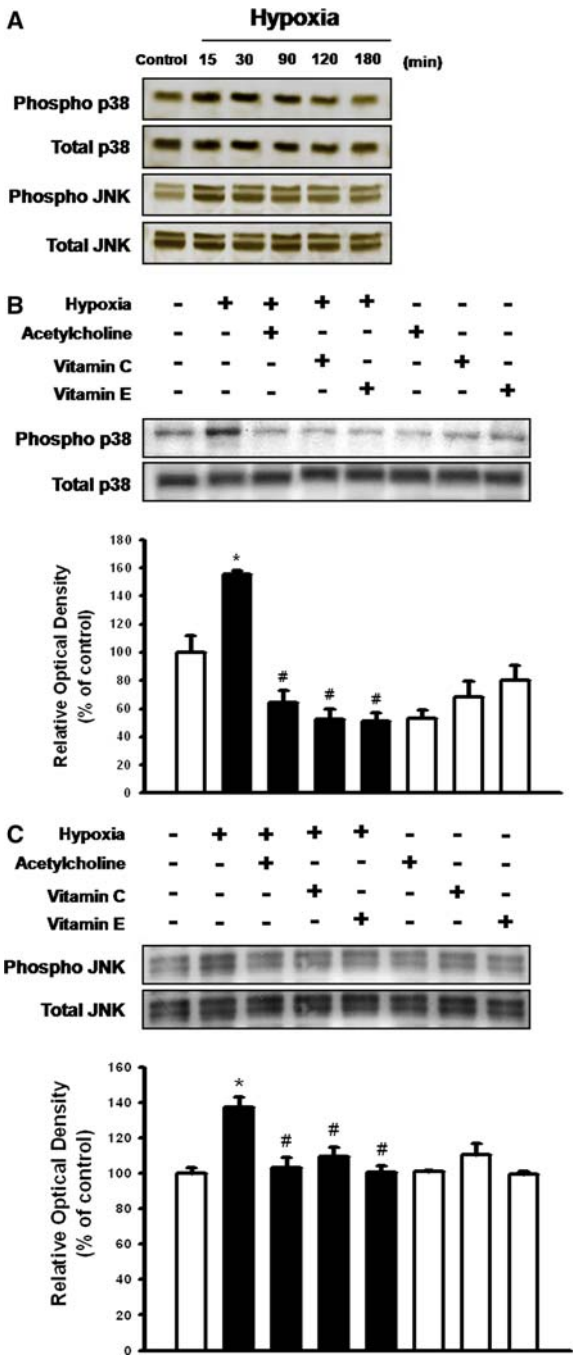

Fig. 4 Effect of ACh on the hypoxia-induced phosphorylation of MAPKs. (**A**) Mouse ES cells were exposed to normoxia or hypoxia for 15–180 min. The phosphorylated p38 MAPK and JNK were then detected, as described in Materials and Methods. The mouse ES cells with or without the ACh pretreatment were exposed to hypoxia for 90 min. Moreover, the cells were pretreated with or without vitamin C (10^{-3} M) and vitamin E (10^{-5} M) for 30 min, and exposed to hypoxia for 90 min (**B**) The phosphorylated p38 MAPK and (**C**) JNK were detected by Western blotting. The values are reported as the mean ± SE of 5 independent experiments. Open bar, control; filled bars, hypoxia. * $P < 0.05$ versus control (normoxia), # $P < 0.05$ versus hypoxia alone

ROS within the confines of the mitochondria. In hypoxia, the loss of membrane potential effectively removes the compartmentalization of ROS to the mitochondria. Rather than increasing total ROS during hypoxia, it is envisioned that cytoplasmic ROS are increased as they are no longer "caged" within the mitochondria [3, 5]. The present results confirmed that hypoxia increases intracellular level of ROS generation, which activates JNK and p38 MAPK as well as the NF-κB pathway in the hypoxia-induced apoptotic response. Consistent with these findings, hypoxia-induced signal molecules have been reported. ROS stimulates cell death or tissue injury directly during hypoxia and reoxygenation via p38 MAPK and JNK [34]. The activation of p38 MAPK and JNK during oxidative stress induce the downstream inducible transcription factor, NF-κB, which binds to a specific promoter region of the tumor necrosis factor (TNF)-α in the nucleus [35]. TNF-α initiates a receptor-dependent death pathway by activating caspases

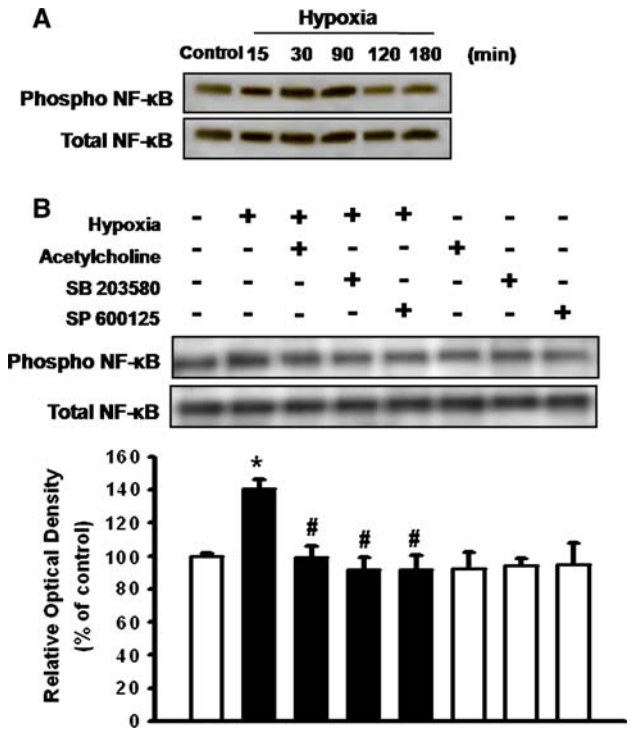

Fig. 5 Effects of ACh on the hypoxia-induced phosphorylation of NF-κB. (**A**) The mouse ES cells were exposed to normoxia or hypoxia for 15–180 min. The phosphorylated NF-κB was detected as described in Materials and methods. (**B**) Mouse ES cells with or without ACh and cells pretreated with SB 203580 (p38 MAPK inhibitor, 10^{-6} M) or SP 600125 (JNK inhibitor, 10^{-6} M) for 30 min were exposed to hypoxia for 90 min and the phosphorylated NF-κB was detected. The values are reported as the mean ± SE of 4 independent experiments. The bands represent 65 kDa of NF-κB. Open bar, control; filled bars, hypoxia. * $P < 0.05$ versus control (normoxia), # $P < 0.05$ versus hypoxia alone

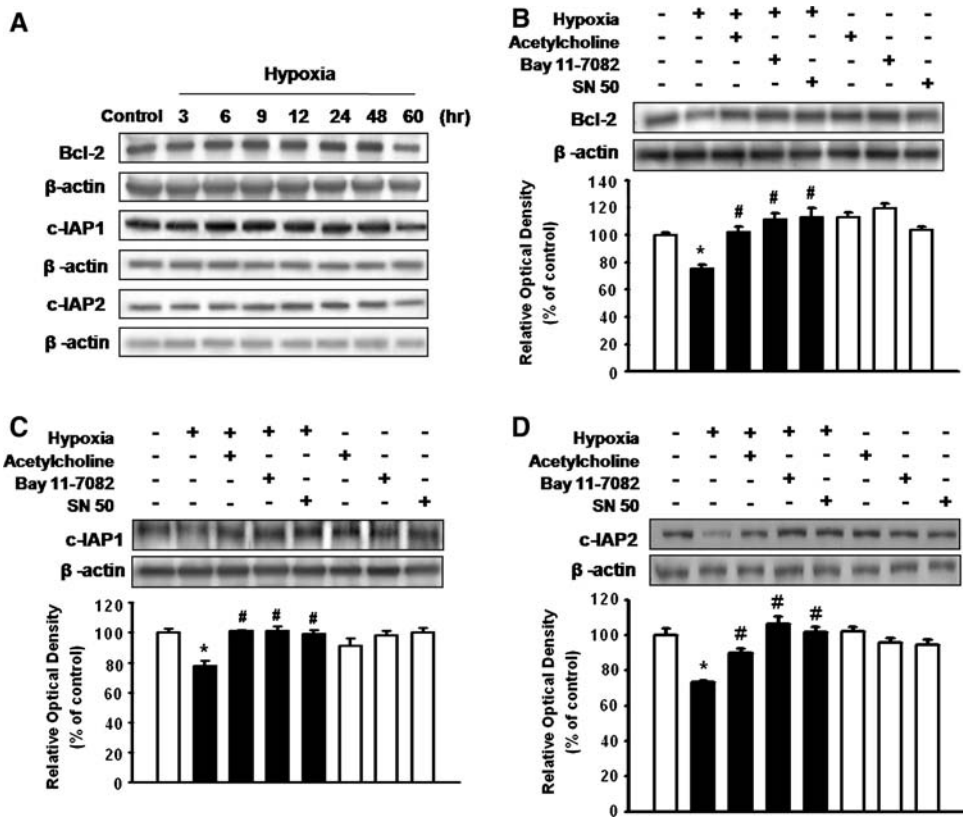

Fig. 6 Effect of ACh on the hypoxia-induced decrease in Bcl-2 and c-IAPs expression. (**A**) The mouse ES cells were exposed to normoxia or hypoxia for 3–60 h and the activated Bcl-2, c-IAP1, and c-IAP2 were detected as described in Materials and methods. The mouse ES cells with or without the ACh pretreatment were exposed to hypoxia for 60 h. Moreover, the mouse ES cells were pretreated with BAY11-7082 (NF-κB inhibitor, 2×10^{-5} M) or SN 50 (NF-κB inhibitor, 500 ng/ml) for 30 min and Bcl-2 (**B**), c-IAP1 (**C**) and c-IAP2 (**D**) were detected. The values are reported as the mean ± SE of 4 independent experiments. The bands represent 29 kDa of Bcl-2, 70 kDa of c-IAP1, 68 kDa of c-IAP2 and 41 kDa of β-actin. Open bar, control; filled bars, hypoxia. * $P < 0.05$ versus control (normoxia), # $P < 0.05$ versus hypoxia alone

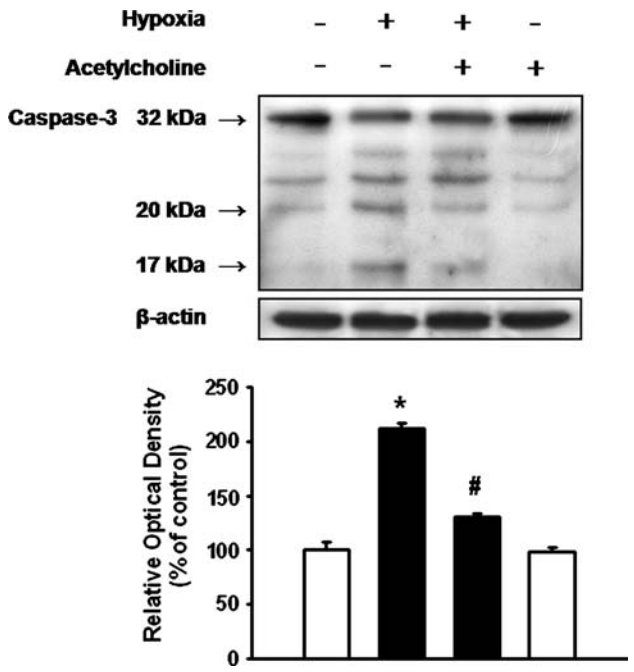

Fig. 7 Effect of ACh on the hypoxia-induced increase in caspase-3 activation. The mouse ES cells with or without ACh were exposed to hypoxia for 60 h and the amounts of the p20 and p17 active subunits and p32 precursor of capase-3 were assessed by Western blotting. The values are reported as the mean ± SE of 4 independent experiments. Open bar, control; filled bars, hypoxia. * $P < 0.05$ versus control (normoxia), # $P < 0.05$ versus hypoxia alone

[36]. In this study, the hypoxia-induced apoptotic pathways were inhibited by ACh through AChR, which suggest that a functional cholinergic system is involved in the anti-apoptotic effect of ACh. It was reported that ACh attenuates oxidative stress and cell death in cardiomyocytes by activating PKC-ε during hypoxic stimulation [28, 33]. Moreover, AChR activation protects the cells from the apoptotic effects including DNA fragmentation, oxidative stress, and mitochondrial dysfunction [31]. AChR has a domain that induces a decrease in oxidative stress sensitivity, possibly playing a role in targeting the antioxidants to specific receptor sites that impart oxidative stress sensitivity [32]. Since mAChR can be identified as G protein-coupled receptor (GPCR), it can be suggested that the anti-oxidative effect of ACh is induced through GPCR-related mechanisms including PLC-linked Ca^{2+} mobilization [37] and cAMP/PKA pathways [38]. AChR also induces the activation of the survival signaling molecules, the increase in the endogenous antioxidant reserve, and the reduction of the apoptotic mediators such as FAS and p38 MAPK during ischemia/reperfusion [39]. Based on these studies, AChR can be speculated to protect oxidative stress though GPCR-mediated mechanisms, although the present study did not show which second molecules are involved in ACh/AChR-mediated anti-oxidative effect or whether ACh/AChR pathway directly regulates specific genes or proteins such as anti-oxidative enzymes.

In this study, an assay to monitor apoptosis and DNA damage in addition to the ES cell viability assay were used to support the finding that ACh blocks the apoptotic cell death induced by hypoxia in mouse ES cells. Caspase-3 has been implicated as a key downstream molecule that executes the apoptotic cascade after hypoxia [34]. In the process of apoptosis-control by caspase, Bcl-2 and IAP play an important role that can protect the cells against apoptosis induced by hypoxia [40]. These results show that a treatment with ACh provides significant protection against the apoptosis-signaling cascade induced by hypoxia. In addition, ACh facilitated the upregulation of the anti-apoptotic Bcl-2 and c-IAPs proteins that suppress effecter caspase activation. Among muscarinic receptors initiating an anti-apoptotic signal, three of which (M1, M3, and M5) are coupled to the $G_{q/11}$-PLC pathway and two (M2 and M4) that inhibit adenylate cyclase via coupling to $G_{i/o}$ [41]. Subsequently, GPCR-linked PI3K/Akt and ERK1/2 pathways inhibit caspase-3 activation [42]. The muscarinic AChR-induced transcription factor such as CREB (cAMP response element-binding) phosphorylation can promote cell survival through the PI3K/Akt pathway to up-regulate the expression of the anti-apoptotic factor Bcl-2 [43, 44]. Another study reported that AChR recovers the expression of Bcl-2 by regulating Bax protein [31]. In the present study, ACh blocked hypoxia-induced NF-κB activation, which decreased Bcl-2 and c-IAPs protein levels. Although the precise intermediate steps between activation of anti-apoptotic pathways and muscarinic receptor-induced ES cell protection await identification, based on previous and our studies, we suggest that the muscarinic pathway has an anti-apoptotic effect through GPCR-linked activation of various survival molecules.

Understanding the biochemical mechanism of this protective response will help in the ultimate goal of determining the physiological importance of ACh in the anti-apoptotic response (Fig. 8). These results do not provide any insights into the mechanistic link between the AChRs and the various signaling pathways examined. Nevertheless, this data at least suggests that the activation of AChRs may play an important role in the hypoxia-induced cell injury/apoptosis by decreasing the level of ROS in ES cells. Therefore, it is suggested that the protection provided by ACh against oxidative stress might be of greater importance in maintaining the function and plasticity of ES, which are likely to be impaired temporally after exposure to hypoxia, even though the indicators of apoptotic signaling were used as the outcome measures in this study. In conclusion, ACh prevents hypoxia-induced mouse ES cell apoptosis through the inhibition of ROS-mediated p38 MAPK and JNK activation as well as the regulation of Bcl-2, c-IAPs, and caspase-3.

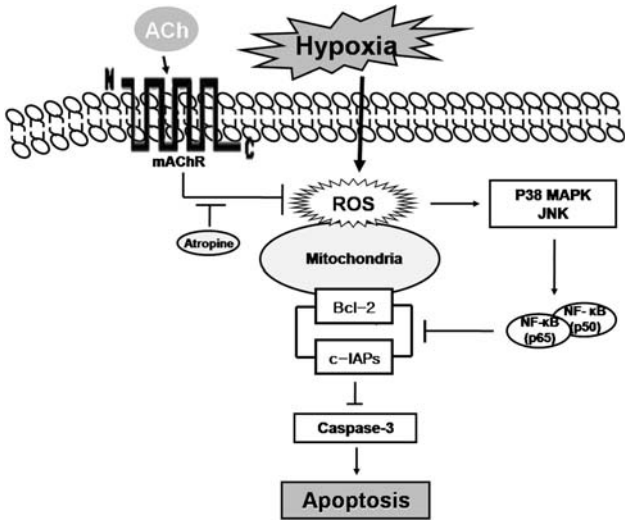

Fig. 8 The hypothesized model for the signal pathways involved in ACh-induced protection of apoptosis by hypoxia in mouse ES cells. Hypoxia increases the generation of ROS, which induce the activation of p38 MAPK and JNK to stimulate NF-κB phosphorylation. Subsequently, the activation of p38 MAPK/JNK and NF-κB inhibits the expression of Bcl-2 and c-IAPs proteins, which block caspase-3. ACh through AChR, which can be blocked by atropine, inhibits the generation of ROS, which in turn blocks hypoxia-induced apoptosis pathways. ACh, Acetylcholine; ROS, reactive oxygen species; MAPK, mitogen-activated protein kinase; JNK, Jun-N-terminal kinase; NF-κB, nuclear factor-κB; c-IAPs, cellular inhibitor of apoptosis proteins

Acknowledgments This research was supported by Grant SC 2210 from the Stem Cell Research Center of the 21st Century Frontier Research Program funded by the Ministry of Science and Technology. We acknowledge a graduate fellowship provided by the Ministry of Education and Human Resources Development through the Brain Korea 21 project, Republic of Korea.

References

1. Zhu LL, Wu LY, Yew DT et al (2005) Effects of hypoxia on the proliferation and differentiation of NSCs. Mol Neurobiol 31:231–242
2. Bunn HF, Poyton RO (1996) Oxygen sensing and molecular adaptation to hypoxia. Physiol Rev 76:839–885
3. Duranteau J, Chandel NS, Kulisz A et al (1998) Intracellular signaling by reactive oxygen species during hypoxia in cardiomyocytes. J Biol Chem 273:11619–11624
4. Vexler ZS, Ferriero DM (2001) Molecular and biochemical mechanisms of perinatal brain injury. Semin Neonatol 6:99–108
5. Millar TM, Phan V, Tibbles LA (2007) ROS generation in endothelial hypoxia and reoxygenation stimulates MAPkinase signaling and kinase-dependent neutrophil recruitment. Free Radic Biol Med 42:1165–1177
6. Grow J, Barks JD (2002) Pathogenesis of hypoxic–ischemic cerebral injury in the term infant: current concepts. Clin Perinatol 29:585–602
7. Johnston MV, Nakajima W, Hagberg H (2002) Mechanisms of hypoxic neurodegeneration in the developing brain. Neuroscientist 8:212–220

8. Santos SC, Vala I, Miguel C et al (2007) Expression and subcellular localization of a novel nuclear acetylcholinesterase protein. J Biol Chem 282:25597–25603
9. Malinger G, Zakut H, Soreq H (1989) Cholinoceptive properties of human primordial, preantral, and antral oocytes: in situ hybridization and biochemical evidence for expression of cholinesterase genes. J Mol Neurosci 1:77–84
10. Paraoanu LE, Steinert G, Klaczinski J et al (2006) On functions of cholinesterases during embryonic development. J Mol Neurosci 30:201–204
11. Wessler I, Kirkpatrick CJ, Racke K (1999) The cholinergic 'pitfall': acetylcholine, a universal cell molecule in biological systems, including humans. Clin Exp Pharmacol Physiol 26:198–205
12. Paraoanu LE, Steinert G, Koehler A et al (2007) Expression and possible functions of the cholinergic system in a murine embryonic stem cell line. Life Sci 80:2375–2379
13. Wessler I, Kirkpatrick CJ, Racke K (1998) Non-neuronal acetylcholine, a locally acting molecule, widely distributed in biological systems: expression and function in humans. Pharmacologist 77:59–79
14. Kawashima K, Fujii T (2004) Expression of non-neuronal acetylcholine in lymphocytes and its contribution to the regulation of immunefunction. Front Biosci 9:2063–2085
15. Dajas-Bailador FA, Lima PA, Wonnacott S (2000) The α7 nicotinic acetylcholine receptor subtype mediates nicotine protection against NMDA excitotoxicity in primary hippocampal cultures through a Ca^{2+} dependent mechanism. Neuropharmacology 39:2799–2807
16. Costa LG, Guizzetti M (1999) Muscarinic cholinergic receptor signal transduction as a potential target for the developmental neurotoxicity of ethanol. Biochem Pharmacol 57:721–726
17. Bhuiyan MB, Murad F, Fant ME (2006) The placental cholinergic system: localization to the cytotrophoblast and modulation of nitric oxide. Cell Commun Signal 4:4
18. Heo JS, Han HJ (2006) ATP stimulates mouse embryonic stem cell proliferation via protein kinase C, phosphatidylinositol 3-kinease/Akt, and mitogen-activated protein kinase signaling pathways. Stem Cells 24:2637–2648
19. Han HJ, Heo JS, Lee YJ (2006) Estradiol-17β stimulates proliferation of mouse embryonic stem cells: involvement of MAPKs and CDK as well as protooncogenes. Am J Physiol Cell Physiol 290:C1067–C1075
20. Lee SH, Heo JS, Han HJ (2007) Effect of hypoxia on 2-deoxyglucose uptake and cell cycle regulatory protein expression of mouse embryonic stem cells: involvement of Ca^{2+}/PKC, MAPKs and HIF-1α. Cell Physiol Biochem 19:269–282
21. Tohgi H, Utsugisawa K, Nagane Y (2000) Hypoxia-induced expression of C1q, a subcomponent of the complement system, in cultured rat PC12 cells. Neurosci Lett 291:151–154
22. Utsugisawa K, Nagane Y, Obara D, Tohgi H (2002) Overexpression of α7 nicotinic acetylcholine receptor prevents G1-arrest and DNA fragmentation in PC12 cells after hypoxia. J Neurochem 81:497–505
23. Chen CH, Ho ML, Chang JK et al (2005) Green tea catechin enhances osteogenesis in a bone marrow mesenchymal stem cell line. Osteoporos Int 16:2039–2045
24. Zhang E, Li X, Zhang S et al (2005) Cell cycle synchronization of embryonic stem cells: effect of serum deprivation on the differentiation of embryonic bodies in vitro. Biochem Biophys Res Commun 333:1171–1177
25. Bradford MM (1976) A rapid and sensitive method for the quantitation of microgram quantities of protein utilizing the principle of protein-dye binding. Anal Biochem 72:248–254
26. Fujii T, Yamada S, Yamaguchi N et al (1995) Species differences in the concentration of acetylcholine, a neruotransmitter, in whole blood and plasma. Neurosci Lett 201:207–210
27. Sastry BVR (1997) Human placentai cholinergic system. Biochem Pharmacol 53:1577–1586
28. Liu H, Bradley C, Zhu X et al (2001) Role of nitric oxide and protein kinase C in Ach-induced cardioprotection. Am J Physiol Heart Circ Physiol 281:191–197
29. Zhang Y, Kakinuma Y, Ando M et al (2006) Acetylcholine inhibits the hypoxia-induced reduction of connexin43 protein in rat cardiomyocytes. J Pharmacol Sci 101:214–222
30. Kakinuma Y, Ando M, Kuwabara M et al (2005) Acetylcholine from vagal stimulation protects cardiomyocytes against ischemia and hypoxia involving additive non-hypoxic induction of HIF-1α. FEBS Lett 579:2111–2118
31. De Sarno P, Shestopal SA, King TD et al (2003) Muscarinic receptor activation protects cells from apoptotic effects of DNA damage, oxidative stress, and mitochondrial inhibition. J Biol Chem 278:11086–11093
32. Joseph JA, Fisher DR, Carey A et al (2004) The M3 muscarinic receptor i3 domain confers oxidative stress protection on calcium regulation in transfected COS-7 cells. Aging Cell 3:263–271
33. McPherson BC, Zhu X, Liu H et al (2002). Acetylcholine attenuates cardiomyocyte oxidant stress during simulated ischemia and reoxygenation. Pharmacology 64:49–56
34. Sun HY, Wang NP, Halkos M et al (2006) Postconditioning attenuates cardiomyocyte apoptosis via inhibition of JNK and p38 mitogen-activated protein kinase signaling pathways. Apoptosis 11:1583–1593
35. Wang T, Zhang X, Li JJ (2002) The role of NF-κB in the regulation of cell stress responses. Int Immunopharmcol 2:1509–1520
36. Zhao ZQ, Vinten-Johansen J (2002) Myocardial apoptosis and ischemic preconditioning. Cardiovasc Res 55:438–455
37. Shinozaki Y, Koizumi S, Ishida S et al (2005) Cytoprotection against oxidative stress-induced damage of astrocytes by extr acellular ATP via P2Y1 receptors. Glia 49:288–300
38. Echeverria V, Clerman A, Dore S (2005) Stimulation of PGE_2 receptors EP2 and EP4 protects cultured neurons against oxidative stress and cell death following β-amyloid exposure. Eur J Neurosci 22:2199–2206
39. Yang B, Lin H, Xu C et al (2005) Choline produces cytoprotective effects against ischemic myocardial injuries: Evidence for the role of cardiac M3 subtype muscarinic acetylcholine receptors. Cell Physiol Biochem 16:163–174
40. Moon DO, Park SY, Heo MS et al (2006) Key regulators in bee venom-induced apoptosis are Bcl-2 and caspase-3 in human leukemic U937 cells through downregulation of ERK and Akt. Int Immunopharmacol 6:1796–1807
41. Caulfield MP (1993) Muscarnic receptors—characterization, coupling, and function. Pharmacol Ther 58:319–379
42. Cui QL, Fogle E, Almazan G (2006) Muscarinic acetylcholine receptors mediate oligodendrocyte progenitor survival through Src-like tyrosine kinases and PI3K/Akt pathways. Neurochem Int 48:383–393
43. Sato-Bigbee C, Pal S, Chu AK (1999) Different neuroligands and signal transduction pathways stimulate CREB phosphorylation at specific developmental stages along oligodendrocyte differentiation. J Neurochem 72:139–147
44. Pugazhenthi S, Nesterova A, Sableet C et al (2000) Akt/protein kinase B up-regulates Bcl-2 expression through cAMP-response element-binding protein. J Biol Chem 275:10761–10766